Afro-Asian Journal of Scientific Research (AAJSR)
المجلة الأفروآسيوية للبحث العلمي
E-ISSN: 2959-6505
Volume 3, Issue 4, 2025
Page No: 259-267
Website: https://aajsr.com/index.php/aajsr/index
SJIFactor 2024: 5.028 ISI 2025: 0.915 معامل التأثير العربي (AIF) 2025: 0.76

Analysis the Impact of Void Defect Position and Size on Medium Voltage PILC Cable

Mohamed Alsharif[1*], Ibrahim Naser[2], Musbah Jbril[3], Abdulgader Alsharif[4]
[1]Department of Communications Engineering and Aviation Information Technology, Technical College of Civil Aviation and Meteorology, Espiaa, Libya
[2]Department of Renewables Energy Engineering, Faculty of Engineering, Sebha University, Sebha, Libya
[3,4]Department of Electric and Electronic Engineering, College of Technical Sciences, Sebha, Libya

تحليل تأثير مكان الفجوة وحجمها على كابلات الجهد المتوسط ذات العازل الورقي المشبع بالزيت

محمد ابوبكر الشريف[1*]، ابراهيم سليمان نصر[2]، مصباح محمد جبريل[3]، عبد القادر الشريف[4]
[1]قسم هندسة الاتصالات وتقنية معلومات الطيران، كلية تقنية الطيران المدني والأرصاد الجوية، اسبيعة، ليبيا
[2]قسم هندسة الطاقة المتجددة، كلية الهندسة جامعة سبها، ليبيا
[4،3]قسم الهندسة الكهربائية و الالكترونية، كلية العلوم التقنية، سبها، ليبيا

*Corresponding author: m.charif@yahoo.com

Received: October 11, 2025 | Accepted: December 22, 2025 | Published: December 30, 2025

Abstract:
Worldwide, most medium-voltage paper-insulated lead-covered cables are operating beyond their intended design life, increasing the likelihood of failure. Irregular electric field distribution over the insulation material causes partial discharge degradation, which reduces the cable's efficiency. Online partial discharge monitoring is used to evaluate the health condition of medium-voltage underground cables. Online partial discharge behaviour detection is highly sensitive to variations in the electric field distribution within three phase medium-voltage cable insulation. The analysis of partial discharge phenomena in medium-voltage cables is mainly based on electric field analysis. Analysing online partial discharge characteristics requires a deep understanding of partial discharge behaviour in insulation systems. The initiation and propagation of partial discharge activity are subject to the critical electric field across the degradation of voids within the cable insulation. This paper presents a study of the electrostatic consequences of void defects and considers the likelihood of internal partial discharge occurring within these defects based on their position and size in belted medium-voltage cables. The nature of the electric field distribution in the cable is presented through finite element analysis. The electric stress variation across different air-filled void defect sizes at multiple positions within the insulation of 11 kV three-phase paper-insulated lead-covered belted cables under online in-service conditions is analysed. The findings contribute to a better understanding of partial discharge behaviour in three-phase medium-voltage cables, enabling enhanced evaluation of asset condition and effective extension of operational lifespan.

Keywords: Medium voltage PILC underground cable, Partial discharge, Finite element analysis, Electric field intensity, Void-defect.

الملخص
عالميًا، تعمل غالبية الكابلات الأرضية الشريطية ثلاثية الطور متوسطة الجهد، ذات العازل الورقي المشبع بالزيت، رغم تجاوز عمرها التصميمي المحدد، مما يزيد من احتمالية حدوث الأعطال. إن التوزيع غير المنتظم للمجال الكهربائي عبر

العزل يؤدي إلى نشوء التفريغ الجزئي الكهربائي، مما يُقلل من كفاءة الكابل. تُستخدم مراقبة التفريغ الجزئي الكهربائي أثناء التشغيل لتقييم الحالة التشغيلية لكابلات الجهد المتوسط الأرضية. يُعد الكشف عن سلوك التفريغ الجزئي الكهربائي أثناء التشغيل حساسًا تجاه التغير المستمر في توزيع المجال الكهربائي داخل نظام العزل في كابلات الجهد المتوسط ثلاثية الطور. يعتمد تحليل ظواهر التفريغ الجزئي في كابلات الجهد المتوسط بشكل رئيسي على تحليل المجال الكهربائي لها. يتطلب تحليل خصائص التفريغ الجزئي الكهربائي أثناء التشغيل فهماً عميقاً لسلوك التفريغ الجزئي في أنظمة العزل. إن بدء وانتشار نشاط التفريغ الجزئي يخضع للمجال الكهربائي الحرج عبر الفراغات داخل العزل. يتناول العمل المقدم في هذه الورقة دراسة الآثار الكهروستاتيكية للفجوات الهوائية داخل عزل كابلات الجهد المتوسط، مع التركيز على تأثير كل من حجم الفجوة وموقعها على نشوء التفريغ الجزئي تحت ظروف التشغيل الفعلية. وباستخدام طريقة العناصر المحدودة، تم تحليل توزيع المجال الكهربائي داخل الكابل، وحساب تغير الإجهاد الكهربائي الناتج عن وجود الفجوات داخل عزل الكابلات الأرضية الشريطية ثلاثية الطور بجهد 11 كيلو فولت. تُسهم هذه النتائج في تعميق الفهم المتعلق بسلوك التفريغ الجزئي في كابلات الجهد المتوسط ثلاثية الطور، وتحسين دقة تقييم سلامة المنظومة، مما يدعم إمكانية إطالة العمر التشغيلي للكابلات بشكل فعّال.

الكلمات المفتاحية: الإجهاد الكهربائي، التفريغ الجزئي الكهربائي، الفجوات الهوائية، كابلات الجهد المتوسط الأرضية ذات العزل الورقي المشبع بالزيت، طريقة العناصر المحدودة.

Introduction

Worldwide, most Medium Voltage (MV) underground cables that were installed are paper-insulated lead-covered (PILC) cables [1, 2]. According to the recommendations of cable manufacturers, the expected lifespan of PILC cables is 40 years [3, 4]. However, many of these cables have been in service for 60 years or more and are now operating beyond their lifespan; therefore, failures are likely to increase [5, 6]. Over time, thermal and electrical operational stresses can lead to partial discharge (PD) activity, which may cause failure of the cable insulation. Partial discharge within cable insulation typically leads to a gradual degradation process that can continue for years before eventually resulting in critical failure and disrupting the power supply to consumers. Interpreting PD activities from online systems should differ from offline PD measurement because during online monitoring (a) all three phases are energized therefore the electric field rotates with power frequency while in off-line test only one phase is energized at a time; (b) the cables are disconnected from the network during off-line test resulting in signal reflections; this does not happen when on-line PD monitoring systems are adopted as cables remain connected in power network and do not have the discontinuity of impedance at a cable end; (c) only a snapshot of the PD activities may be captured with off-line testing as this type of investigation uses short term testing and (d) because changes in load current which occur during normal operation are not applied during off-line tests; these variations in load current have been shown to result in variations in the cable temperature which, in turn, has been shown to give rise to varying PD patterns.

Several types of cable joints have been found to suffer from deterioration and breakdown caused by various factors, including aging, operational stress, and errors during manufacturing or installation [7]. During operation, cable insulation is subjected to mechanical, thermal, and electrical stresses, which over time may induce degradation resulting from alterations in the cable's physical and chemical characteristics. It is well understood that degradation regardless of its specific cause leads to the generation of partial discharges (PDs) at the affected locations. The PDs are small electrical discharges that occur due to localized intensification of the electric field at the fault. Such discharges within or along the surface of insulating materials are typically triggered by highly non-uniform electric fields, which often result from imperfections such as voids, air bubbles, or other structural defects. These imperfections have been identified as the primary sources of PD activity [8, 9].

Charge redistribution in the solid, liquid, or gas causes a spark that produces electrical, mechanical, and thermal stress in the insulation. The signals produced in the PD are determined by the physical conditions and can be used for identifying the presence of the fault. Due to difficulties in making cable connections in outdoor situations, as discussed above, PD usually begins within insulation material of the cable accessories, joints, and terminations. The most common sites for the progressive degradation of the insulation system are the joints [10 – 12] Partial discharge typically occurs in insulation before complete failure. Monitoring PD serves as a crucial tool for identifying potential issues and preventing catastrophic system failure [13]. With effective PD diagnostic systems, it becomes possible to detect some weak spots in cable insulation materials before they lead to a breakdown [14, 15]. In utility operations and industries that use medium-voltage cables, the success of condition-based maintenance depends on continuous monitoring. Online PD-based condition monitoring has become widely adopted [16], and the ability to identify faults within the enclosed structures of cables and joints through remote monitoring benefits both utilities and customers. PD monitoring is an effective tool for assessing the

insulation condition of high-voltage equipment and identifying insulation defects to avoid failures in service [7]. It diagnoses early-stage faults before any significant damage occurs [15].

However, online PD monitoring has sensitivity limitations in detecting PD due to high noise levels [17]. The detection and localization of partial discharges in a three-phase cable are complicated due to the difficulty in determining which of the three phases influences the PD signal. It is difficult to localize and identify the origin of PD pulses. Understanding PD activity in three-phase PILC cable insulation remains a challenge [18]. Analysing the electric field characteristics of void defects is crucial for understanding PD phenomena [19]. Recent studies [20, 21] show that Void defects greatly influence the distribution of the electrostatic field within the insulation of 11 kV three-phase PILC belted cables, potentially increasing the electric field stress inside the void. The work presented here involves online PD monitoring. This paper investigates the characteristics of electrical signals produced by different void-defect sizes at various positions in the cross-section of a three-phase belted-insulated PILC cable under online three-phase voltage. The occurrence of PD due to significant void defects based on their position and size in this three-phase PILC cable model is investigated. The cable dimensions and characteristics are based on data from a commonly used three-phase 11 kV belted PILC cable, as shown in the Figure 1 [20].

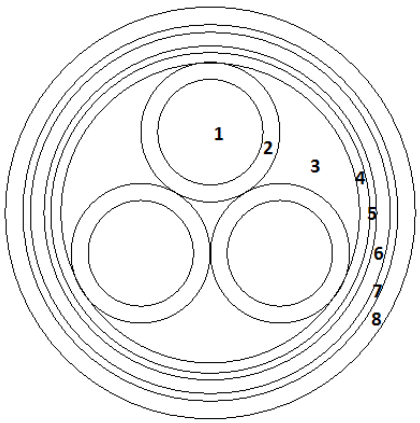

Figure 1: Standard configuration of a three-core 240 mm² PILC cable, showing: (1) copper core, (2) paper insulation saturated with compound, (3) filler material, (4) belted insulation layer, (5) lead covering, (6) bitumen-coated paper layer, (7) steel armouring, and (8) polyvinyl chloride sheath [20].

Methodology

Partial discharge inception field

Most insulation system failures are caused by partial discharges that are preceded by electric field breakdown. [22, 23]. PD generally arises when the dielectric strength of the cable insulation cannot withstand the electric stress applied during high-voltage operation [24]. Discharges usually originate in cavities such as air voids**.** As the applied voltage increases, the electric field within the air void also increases, leading to a greater generation of free electrons within the void [8]. The likelihood of a discharge is influenced by several factors, including temperature, pressure, and the geometry, size, and location of the void. PD initiation in medium-voltage cable insulation depends on the critical electric stress across the void; therefore, PD occurrence in MV cable insulation can be characterized by the partial discharge inception electric field (PDIE).

The breakdown strength of an air-void defect depends on the void's size and pressure [25]. When the void size reaches a critical threshold, significant PD activity can occur [26]. The Paschen curve in Figure 2 shows that the relationship between the breakdown voltage of an air-void defect at atmospheric pressure and its diameter is approximately linear within a certain region. On the left side of the Paschen curve, an increase in void diameter results in a lower breakdown voltage. In contrast, on the right side of the curve, the breakdown voltage rises as the void diameter becomes larger. The relationship between the electric field breakdown of an air-void defect and its diameter is inverse in nature [27]. The equations for PDIV and PDIE derived from Paschen's curve are given in equations 4 and 5, respectively.

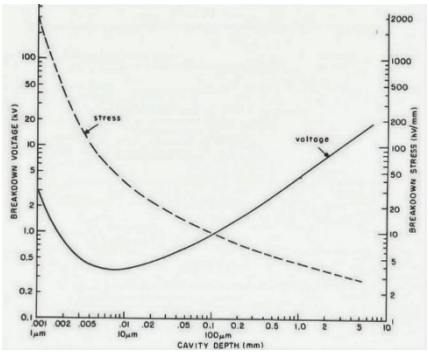

Figure 2: Paschen's curve for air at atmospheric pressure [27].

The electric stress over the void can be obtained by:

$$E = \frac{\Delta V}{d} \qquad (1)$$

$$\Delta V = V_1 - V_2 \qquad (2)$$

The voltage across the void is ΔV , with V_1 and V_2 values dependent on the void's position.

When electrical stress across the void reaches PDIE, the void will discharge and the breakdown electric field (E_b) over the void can be determined by:

$$E_b = \frac{V_b}{d_c} \qquad (3)$$

When $V_b \geq V_{critical}$ and $E_b \geq E_{critical}$

$$V_b = 6.72\sqrt{pd} + 24.36\ pd \qquad (4)$$

Where V b = the breakdown voltage of the void which allows PD to occur in kV (peak).
p = 1 atmospheric pressure in the void.
d = depth of the void in cm.
The void critical electric field $E_{critical}$ that allows PD to occur or PDIE can be obtained from Paschen's Law based on equation 4 as: [28 – 30].

$$E_{critical} = 6.72\sqrt{p/d} + 24.36\ p \qquad (5)$$

The critical size of an air-void,to allow discharge to occur can be written as: d_c

$$d_c = \frac{V_b}{E_b} \qquad (6)$$

Modelling of electric field

The electric field of a standard energized, buried 3-phase 11 kV PILC belted cable is developed, and finite element modelling in COMSOL software is used to study the cable under both defective and non-defective insulation conditions. The Electrostatics module addresses the Poisson's equation as follows:

$$-\nabla\cdot(\varepsilon\nabla V) = -\nabla\cdot\left(\varepsilon_0\varepsilon_r\nabla V\right) = \rho \qquad (7)$$

The density of charge ρ .

By applying the negative gradient of the potential, the electric field intensity is determined as:

$$E = -\nabla V \qquad (8)$$

The distribution of the electric field in the cable cross-section is determined over a single AC cycle of the applied 50 Hz voltage. An 11 kV voltage is applied to the three conductors, while the outer sheath

is grounded at 0 V. The electric field is evaluated in two dimensions for the intact system configuration, providing a baseline for future study. Internal air void defects are introduced into the insulation system to assess changes in electric field stresses. The electric stress within the void is determined using Equation 1.

Void positions

As spherical void defects are common in insulation materials [31, 32], two-dimensional spherical air-void models have been incorporated into the cross-sections of PILC cable insulation. Void-defect sizes were selected based on typical sizes found in the insulation systems of electrical apparatuses in practice. The selected void diameters for partial discharge investigation are 0.3 mm, 0.5 mm, 1 mm, 2 mm, and 3 mm, to evaluate the effects of electrical stress levels on medium-voltage insulation [32]. The void-defect sizes were chosen in accordance with practical void defects reported in references [33 – 36] The void-defect map is defined by the coordinates x and y within the cable insulation cross-sectional domain, with respect to electric field variations across the medium-voltage cable insulation [20]. In the 3-phase PILC belted cable cross-section shown in Figure 3, impregnated oil-paper with a relative permittivity of 4 is used for the insulation layers, including the conductor, filler, and belt.

Taking into account the cable's symmetrical structure, the investigation concentrates on selected void-defect positions. Air-filled voids are introduced at ten locations within the cross-section: five along a circular path and five along a vertical path, each corresponding to different electric field intensities. First, five voids are placed between the phase conductor and the grounded sheath along a circular arc at angular positions of 0°, 15°, 30°, 45°, and 60°. Second, five additional voids are introduced at vertical positions 1, 2, 3, 4, and 5. Based on the cable's symmetrical layout, these positions correspond to equivalent locations throughout the remaining cable region.

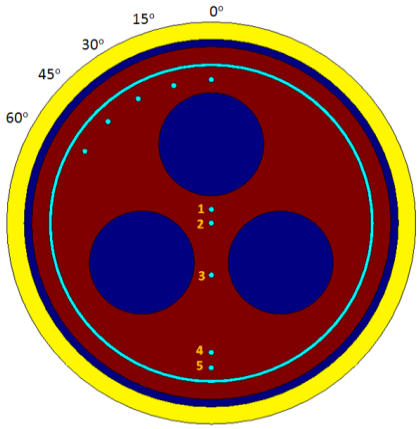

Figure 3: Cross-sectional representation of the PILC cable in the XY coordinate plane, with internal air voids arranged along circular path positions at angles of 0°, 15°, 30°, 45°, and 60°, and at vertical positions 1, 2, 3, 4, and 5.

Results and analysis

Analysis of partial discharge considering the size and position of the void defect

The analyses of PD phenomena focus on variations occurring within a single AC cycle lasting 20 ms. The highest electrical stress within air-filled voids of sizes 0.3, 0.5, 1, 2, and 3 millimetres, at the void positions shown in Figure 3, was determined. The locations of the voids (or their centres) remained constant, while their sizes varied. The procedure was applied across a range of voltage magnitudes in the three-phase cable. The void electric field was calculated using equation 1 and the PDIE was determined using equation 5, both expressed in kV/mm (peak) at an atmospheric pressure of 1 atm. Figures 4 and 5, and Tables 1 and 2, presented the maximum values of the electric field and partial discharge inception field in the void over an AC cycle.

In voids at vertical positions (1, 2, 3, 4, and 5), as shown in Figure 3, the maximum values of the electric field and partial discharge inception field for different void sizes over an AC cycle have been determined. The results are presented in Table 1 and Figure 4. The electric field within the various void-defect sizes is highest at positions 1 and 3 and decreases gradually at positions 2, 4, and 5. At all positions, the highest electric field magnitude is observed for a void size of 0.3 mm, while the lowest occurs at a void size of 3 mm. The electric stress within the void defect gradually decreases as the defect size increases from 0.3 mm to 3 mm. Additionally, larger void sizes correspond to lower electric stress values. This occurs as a result of the decreased effective void dimension (d), as described by

the equation E= ΔV/d, leading to reduced electric stress within the void. Moreover, although the diameter of the void (d) increases, the maximum electric potential difference across the void (V) also increases, making the effect of void size (d) more pronounced. This is in agreement with Paschen's curve in Figure 2, which shows that the breakdown electric stress decreases almost linearly as the void depth increases, whereas the breakdown voltage increases. It is also consistent with similar work on 11kV XLPE cable [32].

The results demonstrate that the electric stresses for different void-defect sizes located in high electric field regions (positions 1 and 3) are higher than those located in low electric field regions (positions 2, 4, and 5). The highest electric stresses are measured for different void-defect sizes at position 3. This is because the maximum electric potential difference across the different void-defect sizes at position 3 situated between two conductors is higher than that across void defects of the same sizes at positions 1, 2, 4, and 5. It can be seen from Figure 4 that there is a probability of PD occurrence within various void-defect sizes in the 11 kV PILC cable insulation at positions 3 and 1, due to their higher electric stress, which exceeds the PDIE according to the Paschen curve. Partial discharge is unlikely to occur in void defects of different sizes situated in low electric field regions, i.e., positions 2, 4, and 5. This is due to the lower electric potential across those void sizes, resulting in lower electric stress.

Table 1: Maximum values of the electric field and partial discharge inception field (kV/mm) for different void sizes (mm) at vertical positions 1, 2, 3, 4, and 5, as shown in Figure 3.

Void size	P 1	P 2	P 3	P 4	P 5	PDIE
0.3	5.3618	3.7611	7.2549	0.7604	0.7316	5.1834
0.5	5.3493	3.7592	7.2356	0.7599	0.7308	4.7891
1	5.3060	3.7436	7.1621	0.7579	0.7265	4.3954
2	5.1323	3.6885	6.8795	0.7501	0.7096	4.1178
3	4.8370	3.5943	6.4383	0.7372	0.6819	3.9949

Figure 4 presents the results of the maximum values of the electric field and the partial discharge inception field for different void sizes of 0.3, 0.5, 1, 2, and 3 millimetres at vertical positions 1, 2, 3, 4, and 5, as shown in Figure 3.

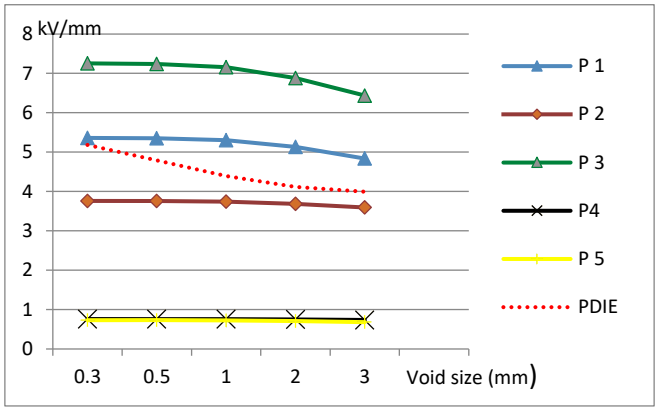

Figure 4: Peak electric field corresponding to various void-defect sizes, located at positions one, two, three, four, and five in Figure 3, and PDIE (dashed line).

Considering the analysis of the other five positions along the circular path, shown in Figure 3 as constructed at angles of 0°, 15°, 30°, 45°, and 60°, the results are presented in Table 2 and Figure 5. The electric field within the void defects was found to decrease gradually at positions 0°, 15°, 30°, 45°, and 60°, respectively, demonstrating the symmetry of the electric field distribution around the phase-voltage conductor. As in the case of the vertical positions, the highest electric field magnitude is observed for a void size of 0.3 mm, while the lowest occurs at a void size of 3 mm across all positions. The electric stress across all void-defect positions gradually decreases from the smallest size (0.3 mm) to the largest size (3 mm). This occurs as a result of the decreased effective void dimension (d), as described by the equation E= ΔV/d. The results also indicate that the maximum electric stress for void-defect sizes located closest to the PILC conductor specifically at position 0° is higher than that of voids located farther away (positions 15°, 30°, 45°, and 60°). This is because the electric potential difference across voids near the conductor is greater than across those located farther away. Partial discharge is

most likely to occur in void-defect sizes at position 0°, where the critical electric field required to initiate PD is reached. In contrast, PD is unlikely to occur in voids located at positions 15°, 30°, 45°, or 60°, where the background electric field is relatively low.

Table 2: Maximum values of the electric field and partial discharge inception field (kV/mm) for different void sizes (mm) at circular positions with angles of 0°, 15°, 30°, 45°, and 60°, as shown in Figure 3.

Void size	P 0º	P 15º	P 30º	P 45º	P 60º	PDIE
0.3	5.4948	4.4159	2.5629	1.4185	0.8475	5.1834
0.5	5.4750	4.4046	2.5605	1.4159	0.8471	4.7891
1	5.3805	4.2420	2.5411	1.4095	0.8419	4.3954
2	5.0041	3.9592	2.4810	1.3830	0.7499	4.1178
3	4.4457	3.8178	2.3843	1.3441	0.7292	3.9949

Figure 5 presents the results of the maximum values of the electric field and the partial discharge inception field for different void sizes of 0.3, 0.5, 1, 2, and 3 at circular positions 0°, 15°, 30°, 45°, and 60°, as shown in Figure 3, along with the partial discharge inception field.

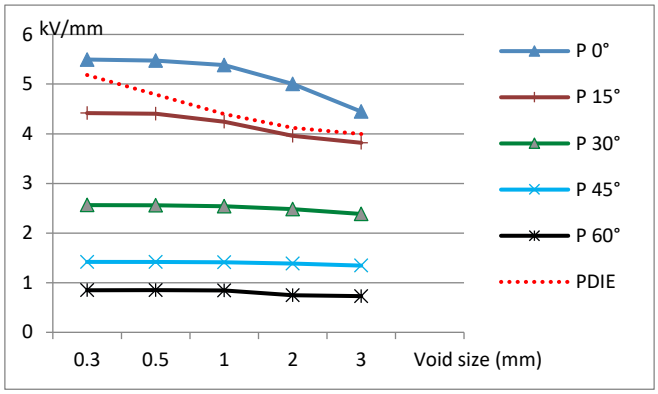

Figure 5: Peak electric field corresponding to various void-defect sizes, located at positions 0^0, 15^0, 30^0, 45^0, and 60^0 of Figure 3 and PDIE (dashed line).

The results demonstrate that void-defect electric stress depends on both the size and position of a void. The smaller the void, the higher the electric stress, and vice versa. Void defects located in regions of strong electric fields, particularly near the conductor, are subjected to greater electric stress. In contrast, voids positioned farther from the conductor, where the electric field is weaker, are less likely to initiate partial discharges. Voids ranging from 0.3 mm to 3 mm, located in high-stress regions such as positions 1, 3, or at 0°, are more likely to initiate partial discharges in 11 kV three-phase PILC cable insulation.

Conclusion

The electric field modelling of an 11-kV paper-insulated, lead-covered belted cable considering various positions and sizes of void defects under a three-phase voltage system was analysed using the finite element method. The influence of voids on the electrostatic characteristics of PILC cable insulation was investigated, and the impact of electric stress caused by different void-defect sizes and positions in medium-voltage PILC-insulated cables was presented. Void defects located in regions with a high background electric field experience greater electric stress, while those in areas with lower electric field strength experience less. Smaller voids also produce higher electric stress levels than larger ones. Variations in electric stress play a critical role in the initiation of partial discharges. The size and position of voids are key factors in determining the intensity of electric stress, which directly affects the likelihood of partial discharge.

References

[1] Bezprozvannych, G.V. & Moskvitin, Y.S. (2023). *Physical processes of aging and assessment of the technical condition of power cables with paper-impregnated insulation*. In: 2023 IEEE 4th KhPI Week on Advanced Technology (KhPIWeek), Kharkiv, Ukraine, pp. 1–5.

[2] Mladenovic, I. & Weindl, C. (2012). *Empiric approach for criteria determination of remaining lifetime*. Dielectric Material, p.251.

[3] Zarim, Z.A.A. & Anthony, T.M. (2012). *Development of remaining life estimation for MV PILC due to electrical stress using statistical method*. In: 2012 IEEE International Conference on Condition Monitoring and Diagnosis, Bali, Indonesia, pp. 1151–1155.
[4] Zapf, M., Blenk, T., Müller, A.C., Pengg, H., Mladenovic, I. & Weindl, C. (2021). *Lifetime assessment of PILC cables with regard to thermal aging based on a medium voltage distribution network benchmark and representative load scenarios in the course of the expansion of distributed energy resources*. Energies, 14(2), p.494.
[5] Mladenovic, I., Weindl, C. & Scharrer, T. (2013). *Effects of MV PILC cables ageing process on the diagnostic parameters*: P-factor and tanδ. In: 2013 IEEE International Conference on Solid Dielectrics (ICSD), Bologna, Italy, pp. 92–95.
[6] Zhou, C., Yi, H. & Dong, X. (2017). *Review of recent research towards power cable life cycle management*. High Voltage, 2(3), pp.179–187.
[7] Veen, J. (2005). *On-line signal analysis of partial discharges in medium voltage power cables*. (Doctoral dissertation, Technische Universiteit Eindhoven) Technische Universiteit Eindhoven.
[8] Illias, H.A., Tunio, M.A., Bakar, A.H.A., Mokhlis, H. & Chen, G. (2016). *Partial discharge phenomena within an artificial void in cable insulation geometry: experimental validation and simulation*. IEEE Transactions on Dielectrics and Electrical Insulation, 23(1), pp. 451–459.
[9] AlShaikh Saleh, M., Refaat, S.S., Olesz, M., Abu-Rub, H. & Guziński, J. (2021). *The effect of protrusions on the initiation of partial discharges in XLPE high voltage cables*. Bulletin of the Polish Academy of Sciences. Technical Sciences, 69.
[10] Gulski, E., Smit, J.J. & Wester, F.J. (2005). *PD knowledge rules for insulation condition assessment of distribution power cables*. IEEE Transactions on Dielectrics and Electrical Insulation, 12(2), pp. 223–239.
[11] Tian, Y., Lewin, P.L. & Davies, A.E.(2002). *Comparison of on-line partial discharge methods for HV cable joints detection*. IEEE Transactions on Dielectrics Electrical Insulation, 9(4), pp. 604–615.
[12] Schichler, U. (1997). *A sensitive method for on-site partial discharge detection on XLPE cable joints*. In: Proceedings of the 5th International Conference on Properties and Applications of Dielectric Materials, 25-30 May 1997, Seoul, Korea, pp. 1099–1102.
[13] Babnik,T., Aggarwal, R.K., Moore, P.J. & Wang, Z.D. (2003*). Radio frequency measurement of different discharges*. In:IEEE Power Tech Conference, 23–26 June 2003, Bologna, Italy, pp.1–5.
[14] Van der Wielen, P.C.J.M. (2005). *On-line detection and location of partial discharges in medium-voltage power cables*. (Doctoral dissertation, Technische Universiteit Eindhoven) Technische Universiteit Eindhoven.
[15] Cuppen, A.N., Steennis, E.F. & Van der Wielen, P.C.J.M. (2010). *Partial discharge trends in medium voltage cables measured while in-service with PDOL*. In: IEEE PES Transmission and Distribution Conference and Exposition, New Orleans, LA, USA, pp. 1–5.
[16] Raymond, W.J.K., Illias, H.A. & Mokhlis, H. (2015). *Partial discharge classifications: Review of recent progress. Measurement*, 68, pp. 164–181.
[17] Hussain, G.A., Hassan, W., Mahmood, F., Shafiq, M., Rehman, H. & Kay, J.A. (2023). *Review on partial discharge diagnostic techniques for high voltage equipment in power systems*. IEEE Access, 11, pp.51382-51394.
[18] Hunter, J.A., Lewin, P.L., Hao, L., Walton, C. & Michel, M. (2013). *Autonomous classification of PD sources within three-phase 11 kV PILC cables*. IEEE Transactions on Dielectrics and Electrical Insulation, 20(6), pp. 2117–2124.
[19] Sun, Y., Lv, A. & Xie, Z. (2024) *Analysis of electric field and partial discharge characteristics of cable joint stress cone dislocation defects*. IET Science, Measurement & Technology, 18(5), pp. 231–244.
[20] Alsharif, M.A. & Naser, I.S. (2020). *Partial discharge activity in PILC belted medium voltage cable*. The Journal of Pure and Applied Sciences (JOPAS), ISSN: 2521-9200.
[21] Alsharif, M., Wallace, P. A., Hepburn, D. M., & Zhou, C. (2015*). Electric Field Investigation in MV PILC Cables with Void Defect.*, International Conference on Power and Energy Systems Engineering (ICPESE). Dubai, UAE.
[22] Halim, H.S.A. & Ghosh, P. (2008). *Condition assessment of medium voltage underground PILC cables using partial discharge mapping and polarization index test results*. In: International Symposium on Electrical Insulation, 9–12 June 2008, Vancouver, Canada, pp. 32–35.
[23] Kando, M. (1992). *Partial discharges using a zero cross AC voltage.* In: Sixth International Conference on Dielectric Materials, Measurements and Applications, 7–10 September 1992, Manchester, UK, pp. 354–357.

[24] Boggs, S. & Densley, J. (2000). *Fundamentals of partial discharge in the context of field cable testing*. IEEE Electrical Insulation Magazine, 16(5), pp. 13–18.
[25] Kreuger, F.H., (1989). *Partial discharge detection in high voltage equipment*. London: Butterworths.
[26] Gouda, O.E., ElFarskoury, A.A., Elsinnary, A.R. & Farag, A.A. (2018). *Investigating the effect of cavity size within medium-voltage power cable on partial discharge behaviour*. IET Generation, Transmission & Distribution, 12(5), pp. 1190–1197.
[27] Bartnikas, R. & McMahon, E.J. (1979). *Engineering dielectrics, volume I, corona measurement and interpretation*. ASTM Special Technical Publication.
[28] Kuffel, E., Zaengl, W.S. & Kuffel, J. (2000). *High Voltage Engineering Fundamentals*. 2nd ed. Oxford: Butterworth-Heinemann.
[29] Radmilovic-Radjenovic, M., Radjenovic, B., Bojarov, A., Klas, M. & Matejcik, S. (2013). *The breakdown mechanisms in electrical discharges*: The role of the field emission effect in direct current discharges in micro gaps. Acta Physica Slovaca, 63.
[30] Kacprzyk, R. & Miśta, W.(2006). *The surface potential of perforated dielectric layers*. IEEE Transactions on Dielectrics and Electrical Insulation,13(5), pp. 986–991.
[31] Illias, H.A., Chen, G. & Lewin, P.L. (2009). *Modelling of partial discharge activity in different spherical cavity sizes and locations within a dielectric insulation material*. In: 9th International Conference on the Properties and Applications of Dielectric Materials, 19–23 July 2009, Harbin, China, pp. 484–488.
[32] Alsharif, M. & Naser, I.S. (2020). *Study of the impact of void-defect in 11 kV XLPE cable insulation*. International Journal of Scientific & Engineering Research (IJSER), 11(11), pp. 330. ISSN 2229-5518
[33] Wensheng, G., Ning, S. & Qingduo, Y. (2009). *Size effect of partial discharge in solid void defects*. In: 9th International Conference on Properties and Applications of Dielectric Materials, 19–23 July 2009, Harbin, China, pp. 501–504.
[34] Dascalescu, L., Ribardikre, P., Duvanaud, C. & Paillot, J. (1998). *Electrostatic discharges from charged particles approaching a grounded surface*. In: Electrical Overstress/Electrostatic Discharge Symposium Proceedings, 6–8 Oct 1998, Reno, NV, USA, pp. 118–123.
[35] Wester, F.J., Gulski, E. & Smit, J.J. (2007). *Detection of partial discharges at different AC voltage stresses in power cables*. IEEE Electrical Insulation Magazine, 23(4), pp. 28–43.
[36] Musa, U., Mati, A.A., Mas'ud, A.A., Shehu, G.S., Rodríguez-Serna, J.M., Al-Shammari, S.J., Rohani, M.N. & Muhammad-Sukki, F. (2023). *FEA-based simulation of accelerated ageing in a power cable due to sustained partial discharge activities in a spherical cavity*. Arabian Journal for Science and Engineering, 48(11), pp. 15029–15043.